

# Bringing multilevel quantum master equations into Lindblad form for complete positivity tests: Two approaches

Timur V. Tscherbul

Department of Physics, University of Nevada, Reno, Nevada, 89557, USA

While quantum master equations (QMEs) are the primary workhorse in quantum information science, quantum optics, spectroscopy, and quantum thermodynamics, bringing an arbitrary  $N$ -level QME into Lindbladian form and verifying complete positivity of the associated quantum dynamical map remain open challenges for  $N \geq 3$ . We explore and implement two independent methods to accomplish these tasks, which enable one to directly compute the Kossakowski matrix of an arbitrary Markovian QME from its Liouvillian. In the first method, due to Hall, Cresser, Li, and Andersson, the Kossakowski matrix elements are obtained by evaluating the action of the Liouvillian on the orthonormal  $SU(N)$  basis matrices and then computing a sum of matrix-product traces. The second method, developed in this work, is based on the real  $N$ -level coherence vector and relies on the Moore-Penrose pseudo-inverse of a rectangular matrix composed of the structure constants of  $SU(N)$ . We show that both methods give identical results, and apply them to establish the complete positivity of the partial secular Bloch-Redfield QME for the  $\Lambda$  and  $V$ -systems driven by incoherent light. We find that the eigenvalues of the Kossakowski matrix of these seemingly different three-level systems are identical, implying close similarities of their dissipative dynamics. By facilitating the expression of multilevel Markovian QMEs in Lindblad form, our results enable testing the QMEs for complete positivity without solving them, as well as restoring complete positivity by keeping only non-negative eigenvalues of the Kossakowski matrix.

## 1 Introduction

Quantum master equations (QMEs) describe the time evolution of a quantum subsystem of interest coupled to a (typically) much larger environment [1–3]. As such, they play a vital role in many areas of physics and chemistry, where the accurate description of environmental effects on quantum dynamics is essential, such as quantum information science [4–14], quantum optics [2, 15], quantum thermodynamics [16–24], spectroscopy [25–29], and chromophoric energy transport [30–34]. When used within their respective domains of validity, QMEs offer a robust and physically meaningful description of environment-induced relaxation and decoherence in  $N$ -level quantum systems [1–3].

A crucial property of any QME is complete positivity (CP) of the quantum dynamical map associated with it [1–3]. The CP condition requires not only that the reduced dynamics of a subsystem of interest be positive, but also that it remains so when the subsystem is entangled with arbitrary ancillae [1–3]. This condition is a defining property of a quantum channel [3] and its violation can lead to unphysical effects, such as entanglement generation by purely local interactions [35, 36] and violations of the second law of thermodynamics [23, 37]. Given recent advances in quantum thermodynamics [22, 24] and quantum information processing [38, 39] with multilevel quantum systems (qudits), the question of whether the dynamical map generated by a given QME satisfies the CP condition acquires critical importance.

In principle, this question can be resolved by mapping the QME's Liouvillian matrix (expressed in terms of relaxation and decoherence rates) to the so-called Kossakowski matrix  $\mathbf{A}$ , which parametrizes the canonical Gorini-Kossakowski-Lindblad-Sudarshan (GKLS) generator of the quantum dynamical semigroup as

sociated with the QME [1]. The dynamical map is CP if  $\mathbf{A}$  has only nonnegative eigenvalues [1]. The Kossakowski matrix determines the key properties of the quantum dynamical map, and plays an essential role in, e.g., quantifying the extent of non-Markovianity of quantum evolutions [12, 40].

While the analytical mapping between the Liouvillian and Kossakowski matrices is well-established for the two-level system [1], this is not the case for multilevel quantum systems ( $N \geq 3$ ). Although analytic expressions for the relaxation and decoherence rates in terms of the elements of the Kossakowski matrix were obtained for  $N = 3$  [41], these expressions are quite cumbersome [1, p. 69] and have not been inverted to the best of our knowledge. As a result, Kossakowski matrices for  $N \geq 3$  are presently calculated via indirect methods, which are applicable only to specific subclasses of QMEs, such as the secular QME [1] and certain noseccular QMEs of the Bloch-Redfield type, both Markovian and non-Markovian [5, 6, 42–44]. These QMEs are typically expressed in operator form, with the Kossakowski matrices expressed via Fourier transforms of environmental correlation functions. However, a limitation of these approaches is their lack of generality, i.e., it is not always clear whether a given QME can be expressed in one of the prescribed operator forms. Therefore, obtaining the Kossakowski matrix from the Liouvillian of an arbitrary multilevel QME remains an open challenge [1], preventing robust CP testing of the underlying quantum dynamical maps.

In 2007, Andersson, Cresser, and Hall showed that any time-local QME can be decomposed into Kraus operators, and thereby tested for CP by constructing the Choi matrix associated with its Kraus-type representation [45]. Specifically, a quantum dynamical map is CP if and only if the corresponding Choi matrix is positive [45, 46]. This method is applicable to a wide class of QMEs, including non-Markovian QMEs written in a time-local form (which can be obtained from the generalized Nakajima-Zwanzig-type QME via the time-convolutionless projection operator method [47–50]). However, the construction of the Choi matrix and the associated Kraus decomposition requires explicitly solving the QME [45], which can be a computationally intensive task for multilevel QMEs. As

such, its applications have been limited to two-level systems [45].

More recently, Hall, Cresser, Li, and Anderson [51] pointed out that the Kossakowski matrix can be obtained by evaluating the action of the Liouvillian on the basis matrices of  $SU(N)$ , and then computing the trace of a matrix product, as given by Eq. (A7) of Ref. [51]. However, the computational significance of this result has remained unexplored. In particular, to the author’s knowledge, it has not been applied to calculate the Kossakowski matrices of multilevel ( $N \geq 3$ ) systems.

Here, we show that the approach of Ref. [51] can be used as the basis for an efficient method to calculate the Kossakowski matrices of  $N$ -level Markovian QMEs from their Liouvillians. Focusing on the quantum optical QME of the partial secular Bloch-Redfield (PSBR) type [52–54], which describes multilevel atoms and molecules interacting with incoherent radiation fields, we use the method to calculate the Kossakowski matrix of the PSBR equation for three-level V and  $\Lambda$  systems and show that the corresponding dynamical map is CP. In addition to the method of Ref. [51], which is based on the density matrix formalism, we develop an alternative approach, which relies on the real coherence vector, and show that both approaches give identical results.

The quantum dynamics of multilevel atoms and molecules interacting with incoherent radiation fields (such as sunlight, or, more generally, thermal blackbody radiation) is of paramount importance in a number of research fields, including precision measurement [55, 56], photosynthetic light-harvesting [53, 56–63], and quantum thermodynamics [64, 65]. Interestingly, these dynamics can generate the so-called noise-induced Fano coherences between the nearly degenerate ground and/or excited states of a multilevel quantum system [52–54, 56, 58–66], even when the initial state of the system is coherence-free. The emergence of Fano coherences under incoherent driving is due to the non-secular population-to-coherence coupling terms properly described by the PSBR equation [54, 58–62] but not the simpler secular rate equations. The physical origin of these non-secular terms can be traced back to quantum interference between the different incoherent excitation and relaxation pathways [58, 61].

Far from a mere mathematical curiosity, Fano coherences have a number of experimentally verifiable [59, 62] physical implications. They can strongly affect the thermalization dynamics of a multilevel quantum system interacting with a bath [53, 60, 62], leading to anomalously slow approach to thermal equilibrium which occurs over multiple, often vastly different, timescales [53, 58–62, 67–69]. The resulting coherent steady states can break detailed balance [52, 59, 61, 64] thereby enhancing the efficiency of photovoltaic devices [64]. In addition, closely related pre-thermal states can have promising applications in quantum thermometry [70].

Although the PSBR equation is the main tool, with which non-secular effects and Fano coherences are modeled, it has been an open question whether the time evolution generated by this equation satisfies the CP property [43, 53], calling into question the physical significance of non-secular effects and Fano coherences. Here, we settle this question by using the method of Ref. [51] to explicitly calculate the Kossakowski matrix for the archetypal three-level  $\Lambda$  and V-systems. We show that the eigenvalues of the Kossakowski matrix are non-negative, establishing the CP property of the PSBR dynamical map acting on these systems. Our calculations further show that the eigenvalues of the Kossakowski matrices of the  $\Lambda$  and V-systems are identical, implying close similarities in the dissipative dynamics of these seemingly different systems.

## 2 Theoretical approaches: Extracting the Kossakowski matrix from the Liouvillian

We begin by specifying the general Markovian QME for the reduced density matrix  $\rho$  of an  $N$ -level quantum system described by the Hamiltonian  $\mathbf{H}_S$  interacting with an environment [1, 2]

$$d\rho/dt = \hat{\mathcal{L}}[\rho] = \hat{\mathcal{L}}_H[\rho] + \hat{\mathcal{L}}_D[\rho], \quad (1)$$

where the Liouvillian superoperator  $\hat{\mathcal{L}}$ , assumed here to be time-independent, can be separated into the Hamiltonian ( $\hat{\mathcal{L}}_H[\rho] = -i[\mathbf{H}_S, \rho]$ ) and dissipative parts. The latter can be expressed in

the GKLS form [1]

$$\hat{\mathcal{L}}_D[\rho] = \frac{1}{2} \sum_{i,k=1}^M a_{ik} (2\mathbf{F}_i \rho \mathbf{F}_k - \rho \mathbf{F}_k \mathbf{F}_i - \mathbf{F}_k \mathbf{F}_i \rho), \quad (2)$$

where  $a_{ik}$  are the elements of the Kossakowski matrix  $\mathbf{A}$ , and the basis set  $\{\mathbf{F}_i\}$  is composed of  $M = N^2 - 1$  Hermitian traceless  $N \times N$  matrices, which satisfy  $\text{Tr}(\mathbf{F}_i \mathbf{F}_k^\dagger) = \delta_{ik}$  [1]. For  $N = 3$ , the basis matrices  $\mathbf{F}_i$  correspond to the generators of the SU(3) Lie group, also known as error generators [71]. We follow the standard practice of choosing the  $\mathbf{F}_i$  to be the Gell-Mann matrices [1, 72]. Note that the summation in Eq. (2) does not include the basis matrix  $\mathbf{F}_0$ , which is proportional to the unit matrix, and thus commutes with  $\hat{\rho}$  and the  $\mathbf{F}_k$  ( $k = 1, M$ ), so the terms involving  $\mathbf{F}_0$  evaluate to zero. Our goal is to obtain the matrix elements of  $\mathbf{A}$  in terms of those of the Liouvillian  $\hat{\mathcal{L}}_D$ .

Hall and co-workers derived the following expression for the Kossakowski matrix in terms of the Liouvillian [51], which follows from the proof of Lemma 2.2 of Ref. [73]

$$a_{ij} = \sum_{m=0}^M \text{Tr}(\mathbf{F}_i \mathbf{F}_m \hat{\mathcal{L}}_D[\mathbf{F}_m] \mathbf{F}_j). \quad (3)$$

The calculation of the Kossakowski matrix elements thus requires evaluating the action of the Liouvillian superoperator on the SU( $N$ ) basis matrices (the term  $\hat{\mathcal{L}}_D[\mathbf{F}_m]$ ) followed by the computation of the matrix product trace.

Here, we use Eq. (3) as a basis for calculating the Kossakowski matrices for archetypal three-level V and  $\Lambda$  systems driven by incoherent radiation (see Sec. III below). In principle, however, Eq. (3) is general and can be extended to  $N$ -level systems with  $N \geq 4$  [56] and time-dependent Liouvillians.

As an alternative to Eq. (3), we propose an independent approach to validate our results. The approach is based on the real coherence vector  $\mathbf{v}$  [1], whose components are defined by the SU( $N$ ) decomposition of  $\rho$  [1, 74, 75]

$$\rho(t) = \frac{1}{N} \mathbf{F}_0 + \sum_{i=1}^M v_i(t) \mathbf{F}_i \quad (4)$$

with  $v_i(t) = \text{Tr}(\rho(t) \mathbf{F}_i)$  ( $\mathbf{v}$  is identical to the standard Bloch vector for  $N = 2$  [1]). The real components  $v_i$  satisfy an inhomogeneous QME, which

is equivalent to the original QME [1, 74, 75]

$$\dot{\mathbf{v}}(t) = [\mathbf{Q} + \mathbf{R}] \mathbf{v}(t) + \mathbf{k}, \quad (5)$$

where  $\mathbf{k}$  is the driving vector and the matrix operators  $\mathbf{Q}$  and  $\mathbf{R}$  describe the Hamiltonian and dissipative evolution analogously to  $\hat{\mathcal{L}}_H$  and  $\hat{\mathcal{L}}_D$  in the density matrix formulation.

We can express the elements of  $\mathbf{R}$  and  $\mathbf{k}$  in terms of those of  $\mathbf{A}$  [1, 74, 75]

$$r_{sm} = \sum_{i,k=1}^M \mathcal{T}_{sm,ik} a_{ik} \quad (s, m = 1, \dots, M), \quad (6)$$

$$k_s = \frac{i}{N} \sum_{i,k=1}^M a_{ik} f_{kls} \quad (s = 1, \dots, M), \quad (7)$$

where

$$\mathcal{T}_{sm,ik} = -\frac{1}{4} \sum_{l=1}^M [(f_{mnl} + id_{mnl}) f_{kls} + (f_{klm} - id_{klm}) f_{ils}], \quad (8)$$

is an  $M^2 \times M^2$  transformation tensor  $\mathcal{T}$ , which depends on the symmetric ( $f_{mnl}$ ) and antisymmetric ( $d_{mnl}$ ) structure constants of  $SU(N)$  [1]. To the author's knowledge, this tensor has not been explored beyond the two-level system (some of its properties are derived in Appendix A).

We note that Eqs. (6)-(7) can be viewed as a system of linear equations for the coefficients  $a_{ik}$  with the right-hand side given by the  $r_{sm}$  and  $k_s$ . This system can be solved for the  $a_{ik}$  as described in the Appendix, to give the vectorized Kossakowski matrix  $\mathbf{a} = \text{vec}(\mathbf{A})$

$$\mathbf{a} = \mathbf{T}^+ \mathbf{r}, \quad (9)$$

where  $\mathbf{T}$  is a  $(M^2 + M) \times M^2$  complex rectangular tensor composed of the structure constants of  $SU(N)$  and  $\mathbf{T}^+ = (\mathbf{T}^\dagger \mathbf{T})^{-1} \mathbf{T}^\dagger$  is the Moore-Penrose pseudo-inverse of  $\mathbf{T}$  [76–78].

### 3 Results: Complete positivity of Partial Secular Bloch-Redfield evolution of three-level V and $\Lambda$ systems

We have verified by direct numerical computations that Eqs. (3) and (9) give identical results for the Kossakowski matrix of the three-level V-system. However, the density matrix formulation based on Eq. (3) is more computationally

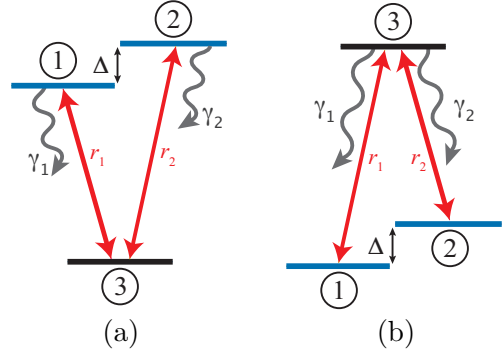


Figure 1: (a) Schematics of three-level V (a) and  $\Lambda$  (b) systems driven by incoherent radiation. The incoherent pumping transitions are denoted by straight lines and spontaneous emission transitions by wavy lines.

efficient because it does not rely on matrix inversion. Here, we use this formulation to establish the CP property of the partial secular Bloch-Redfield equations, which describe the time evolution of Fano coherences in three-level V and  $\Lambda$  systems driven by incoherent radiation.

#### 3.1 V-system

The quantum dynamics of a three-level V-system driven by incoherent blackbody radiation [see Fig. 1(a)] is described by the PSBR equations in the energy basis [54, 58, 79, 80]

$$\begin{aligned} \dot{\rho}_{ii} &= -(r_i + \gamma_i) \rho_{ii} + r_i \rho_{33} - p(\sqrt{r_1 r_2} + \sqrt{\gamma_1 \gamma_2}) \rho_{12}^R, \\ \dot{\rho}_{12} &= -i \rho_{12} \Delta - \frac{1}{2}(r_1 + r_2 + \gamma_1 + \gamma_2) \rho_{12} \\ &\quad + \frac{p}{2} \sqrt{r_1 r_2} (2\rho_{33} - \rho_{11} - \rho_{22}) - \frac{p}{2} \sqrt{\gamma_1 \gamma_2} (\rho_{11} + \rho_{22}), \\ \dot{\rho}_{13} &= -\frac{1}{2}(2r_1 + r_2 + \gamma_1) \rho_{13} - \frac{p}{2} (\sqrt{r_1 r_2} + \sqrt{\gamma_1 \gamma_2}) \rho_{23}, \\ \dot{\rho}_{23} &= -\frac{1}{2}(r_1 + 2r_2 + \gamma_2) \rho_{23} - \frac{p}{2} (\sqrt{r_1 r_2} + \sqrt{\gamma_1 \gamma_2}) \rho_{13}, \end{aligned} \quad (10)$$

where  $i = 1, 2$  denote the excited states of the V-system [see Fig. 1(a)], 3 stands for the ground state,  $r_i$  and  $\gamma_i$  are incoherent absorption and spontaneous emission rates,  $\Delta = \omega_{12}$  is the excited-state energy splitting,  $p = \boldsymbol{\mu}_{31} \cdot \boldsymbol{\mu}_{32} / (|\boldsymbol{\mu}_{31}| |\boldsymbol{\mu}_{32}|)$  quantifies the alignment of transition dipole moments  $\boldsymbol{\mu}_{3i}$ , and  $\rho_{12}^R$  and  $\rho_{12}^I$  denote the real and imaginary parts of  $\rho_{12}$  [52, 53, 58]. Equation (10) is derived in the standard Born-Markov approximation, which is well-justified for multilevel quantum systems interacting with incoherent radiation fields [2, 54]. We retain the nonsecular population-to-coherence coupling terms proportional to  $p$  in Eq. (10),

which are responsible for the generation of noise-induced Fano coherences [52, 53].

To compute the traces of matrix products on the right-hand side of Eq. (3), we need to evaluate the  $N \times N$  matrices  $\mathcal{L}_D[\mathbf{F}_m]$  for the  $N$ -level system of interest. To this end, we express the  $3 \times 3$  density matrix of the V-system as a complex 9-dimensional vector

$$\vec{\rho} = (\rho_{11}, \rho_{22}, \rho_{33}, \rho_{12}, \rho_{21}, \rho_{13}, \rho_{31}, \rho_{23}, \rho_{32})^T, \quad (11)$$

$$\mathcal{L}_D^{(5)} = \begin{pmatrix} -(r_1 + \gamma_1) & 0 & r_1 & \xi_{12}(p) & \xi_{12}(p) \\ 0 & -(r_2 + \gamma_2) & r_2 & \xi_{12}(p) & \xi_{12}(p) \\ r_1 + \gamma_1 & r_2 + \gamma_2 & -(r_1 + r_2) & -2\xi_{12}(p) & -2\xi_{12}(p) \\ \xi_{12}(p) & \xi_{12}(p) & p\sqrt{r_1 r_2} & -\frac{1}{2}(r_1 + r_2 + \gamma_1 + \gamma_2) & 0 \\ \xi_{12}(p) & \xi_{12}(p) & p\sqrt{r_1 r_2} & 0 & -\frac{1}{2}(r_1 + r_2 + \gamma_1 + \gamma_2) \end{pmatrix} \quad (12)$$

where  $\xi_{12}(p) = -\frac{p}{2}(\sqrt{r_1 r_2} + \sqrt{\gamma_1 \gamma_2})$ . In the absence of population-to-coherence coupling terms (the secular limit,  $p = 0$ ), this matrix further

$$\mathcal{L}_D^{(4)} = \begin{pmatrix} -\frac{1}{2}(2r_1 + r_2 + \gamma_1) & 0 & \xi_{12}(p) & 0 \\ 0 & -\frac{1}{2}(2r_1 + r_2 + \gamma_1) & 0 & \xi_{12}(p) \\ \xi_{12}(p) & 0 & -\frac{1}{2}(r_1 + 2r_2 + \gamma_1) & 0 \\ 0 & \xi_{12}(p) & 0 & -\frac{1}{2}(r_1 + 2r_2 + \gamma_1) \end{pmatrix}. \quad (13)$$

Having obtained the matrix representation of the Liouvillian, we can now use Eq. (3) to directly calculate the elements of the Kossakowski matrix for the V-system. To this end, we first define 9-dimensional complex vectors  $\mathbf{f}_i$  by vectorizing the  $SU(N)$  basis matrices (see Sec. II) and then calculate the  $\hat{\mathcal{L}}_D[\mathbf{F}_m]$  as matrix-vector products, i.e.,  $\hat{\mathcal{L}}_D[\mathbf{F}_m] = \mathcal{L}_D \mathbf{f}_m$ . These matrix-vector products are subsequently “devectorized” and used in matrix trace computations to produce the Kossakowski matrix elements, as prescribed by Eq. (3).

### 3.2 $\Lambda$ system

The density matrix of a three-level  $\Lambda$ -system driven by incoherent radiation [see Fig. 1(b)] evolves in time according to the PSBR equation

The Liouvillian then becomes a  $9 \times 9$  supermatrix. The time evolution of state populations  $\rho_{ii}$  and two-photon coherences  $\rho_{12} = \rho_{21}^*$  is decoupled from that of one-photon coherences  $\rho_{13}$  and  $\rho_{23}$  in the partial secular approximation, which is well-justified for the V- and  $\Lambda$  systems considered here [54]. Owing to the partial secular decoupling, the Liouvillian matrix becomes block-diagonal,  $\mathcal{L}_D = \mathcal{L}_D^{(5)} \oplus \mathcal{L}_D^{(4)}$  with the  $5 \times 5$  subblock acting on the top 5 elements of  $\vec{\rho}$  ( $\rho_{11}$ ,  $\rho_{22}$ ,  $\rho_{33}$ ,  $\rho_{12}$ , and  $\rho_{21}$ ) given by

decouples into one  $3 \times 3$  and two  $1 \times 1$  subblocks.

Finally, the  $4 \times 4$  subblock of the Liouvillian matrix that acts on the bottom 4 elements of  $\vec{\rho}$  ( $\rho_{13}$ ,  $\rho_{31}$ ,  $\rho_{23}$ , and  $\rho_{32}$ ) is given by

in the energy basis [54, 62, 81]

$$\begin{aligned} \dot{\rho}_{13} &= -\frac{1}{2}(\gamma_1 + \gamma_2 + 2r_1 + r_2)\rho_{13} - \frac{p}{2}\sqrt{r_1 r_2}\rho_{23}, \\ \dot{\rho}_{23} &= -\frac{1}{2}(\gamma_1 + \gamma_2 + r_1 + 2r_2)\rho_{23} - \frac{p}{2}\sqrt{r_1 r_2}\rho_{13}, \\ \dot{\rho}_{ii} &= -(r_i + \gamma_i)\rho_{ii} + (r_i + \gamma_i)\rho_{33} - p\sqrt{r_1 r_2}\rho_{12}^R, \\ \dot{\rho}_{12} &= -i\rho_{12}\Delta - \frac{1}{2}(r_1 + r_2)\rho_{12} \\ &\quad + p(\sqrt{r_1 r_2} + \sqrt{\gamma_1 \gamma_2})\rho_{33} - \frac{p}{2}\sqrt{r_1 r_2}(\rho_{11} + \rho_{22}), \end{aligned} \quad (14)$$

where  $i = 1, 2$  denote the ground states of the  $\Lambda$ -system [see Fig. 1(a)], 3 stands for the excited state, and the parameters  $r_i$  and  $\gamma_i$  have the same meaning as described below Eq. (10). As in the V-system case considered in the previous section, (i) the population-to-coherence coupling

terms proportional to  $p$  in Eq. (10) are responsible for the generation of noise-induced Fano coherences [62, 81], and (ii) the dynamics of state populations and two-photon coherences is decoupled from that of one-photon coherences  $\rho_{13}$  and  $\rho_{23}$  in the partial secular approximation.

Using the same definition of  $\vec{\rho}$  is in Eq. (11)

$$\mathcal{L}_D^{(5)} = \begin{pmatrix} -r_1 & 0 & r_1 + \gamma_1 & -\frac{p}{2}\sqrt{r_1 r_2} & -\frac{p}{2}\sqrt{r_1 r_2} \\ 0 & -r_2 & r_2 + \gamma_2 & -\frac{p}{2}\sqrt{r_1 r_2} & -\frac{p}{2}\sqrt{r_1 r_2} \\ r_1 & r_2 & -(r_1 + r_2 + \gamma_1 + \gamma_2) & p\sqrt{r_1 r_2} & p\sqrt{r_1 r_2} \\ -\frac{p}{2}\sqrt{r_1 r_2} & -\frac{p}{2}\sqrt{r_1 r_2} & -2\xi_{12}(p) & -\frac{1}{2}(r_1 + r_2) & 0 \\ -\frac{p}{2}\sqrt{r_1 r_2} & -\frac{p}{2}\sqrt{r_1 r_2} & -2\xi_{12}(p) & 0 & -\frac{1}{2}(r_1 + r_2) \end{pmatrix}, \quad (15)$$

where  $\xi_{12}(p) = -\frac{p}{2}(\sqrt{r_1 r_2} + \sqrt{\gamma_1 \gamma_2})$ . In the secular limit ( $p = 0$ ) this matrix further decouples

$$\begin{pmatrix} -\frac{1}{2}(\gamma_1 + \gamma_2 + 2r_1 + r_2) & 0 & -\frac{p}{2}\sqrt{r_1 r_2} & 0 \\ 0 & -\frac{1}{2}(\gamma_1 + \gamma_2 + 2r_1 + r_2) & 0 & -\frac{p}{2}\sqrt{r_1 r_2} \\ -\frac{p}{2}\sqrt{r_1 r_2} & 0 & -\frac{1}{2}(\gamma_1 + \gamma_2 + r_1 + 2r_2) & 0 \\ 0 & -\frac{p}{2}\sqrt{r_1 r_2} & 0 & -\frac{1}{2}(\gamma_1 + \gamma_2 + r_1 + 2r_2) \end{pmatrix}. \quad (16)$$

### 3.3 Kossakowski matrices for three-level $\Lambda$ and V-systems driven by incoherent radiation

Here, we examine the eigenvalues of the Kossakowski matrix of the PSBR equations, which describes the quantum dissipative evolution of the  $\Lambda$  and V-systems driven by isotropic incoherent radiation. Using the approach outlined in Sec. IIA, we found that the eigenvalues calculated for the V system are exactly the same as those for the  $\Lambda$  system in all dynamical regimes spanned by the parameters  $\gamma_1/\gamma_2$ ,  $\bar{n}$ , and  $p$ . This result suggests that quantum dissipative dynamics of  $\Lambda$  and V-systems driven by incoherent radiation can be described by essentially the same diagonal Lindblad equation, and thus can be expected to share closely similar features. This is an example of new insight afforded by the Kossakowski matrix analysis, which is difficult to obtain by examining the (seemingly different) Liouvillians of the V- and  $\Lambda$  systems.

Figure 2 shows the eigenvalues of the Kossakowski matrix for the V and  $\Lambda$ -systems as a function of the ratio of spontaneous decay rates  $\gamma_2/\gamma_1$ , which quantifies the extent of asymme-

[note the different energy level notation in Figs. 1(a) and (b)] and noting that  $\dot{\rho}_{33} = -\dot{\rho}_{11} - \dot{\rho}_{22}$ , the  $9 \times 9$  Liouvillian supermatrix of the  $\Lambda$  system block-diagonalizes into  $5 \times 5$  and  $4 \times 4$  subblocks,  $\mathcal{L}_D = \mathcal{L}_D^{(5)} \oplus \mathcal{L}_D^{(4)}$ , with

into one  $3 \times 3$  and two  $1 \times 1$  subblocks, analogously to the V-system. Finally, the remaining  $4 \times 4$  subblock of the Liouvillian  $\mathcal{L}_D^{(4)}$  becomes

try of two incoherent pumping transitions [58]. Importantly, we observe that the eigenvalues are non-negative across all the regimes studied, which include the weak ( $\bar{n} \ll 1$ ), intermediate ( $\bar{n} = 1$ ), and strong ( $\bar{n} \gg 1$ ) pumping regimes, and transition dipole alignment parameters ranging from  $p = 1$  to  $p = 0$ . This establishes the CP property of the quantum dynamical maps associated with the PSBR equation for three-level V and  $\Lambda$ -systems driven by isotropic incoherent radiation, a central result of this work.

In the weak pumping limit relevant for photosynthetic sunlight-harvesting [53], the incoherent pumping rate is much smaller than that of spontaneous decay ( $\bar{n} \ll 1$ ). Figure 2(a) shows that in this limit, there are only two nonzero eigenvalues for  $p = 1$ , one of which is much larger than the other. Both of the eigenvalues increase monotonically with  $\gamma_1/\gamma_2$ . Four nonzero eigenvalues appear for  $p < 1$ , also increasing steadily with  $\gamma_1/\gamma_2$ . Interestingly, the eigenvalues at  $\gamma_1 = \gamma_2$  experience two genuine crossings in the secular limit ( $p = 0$ ), which become avoided for  $p = 1/2$ .

As shown in Figs. 2(b) and (c), the gap between the eigenvalues closes with increasing

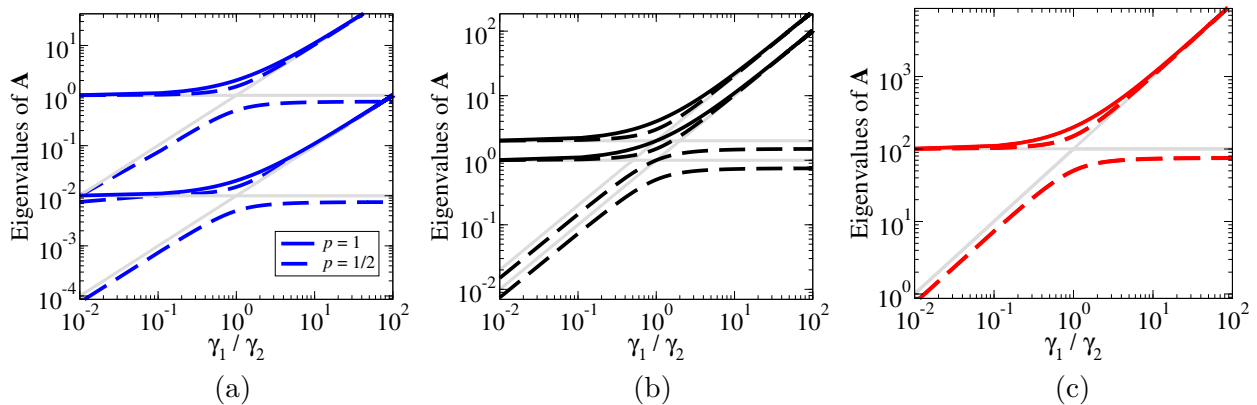


Figure 2: Nonzero eigenvalues of the Kossakowski matrix of the PSBR equation for three-level V- and  $\Lambda$  systems driven by isotropic incoherent radiation. The eigenvalues are plotted as a function of the ratio of spontaneous decay rates  $\gamma_1/\gamma_2$  for collinear transition dipoles ( $p = 1$ , solid lines), perpendicular transition dipoles ( $p = 0$ , solid gray lines), and  $p = 1/2$  (dashed lines) in the weak [ $\bar{n} = 0.01$ , panel (a)], intermediate [ $\bar{n} = 1$ , panel (b)], and strong [ $\bar{n} = 100$ , panel (c)] pumping regimes.

the pumping rate. At  $\bar{n} = 1$  the eigenvalues are within a factor of two of each other, and they become indistinguishable on the scale of Fig. 2(c) at  $\bar{n} = 100$ . The qualitative trends of non-negativity and monotonic increase with the asymmetry parameter  $\gamma_1/\gamma_2$  remain the same as in the weak pumping limit.

## 4 Summary

In summary, we have explored and implemented two direct methods to obtain the Kossakowski matrix of an arbitrary  $N$ -level Markovian QME from its Liouvillian matrix, thereby enabling straightforward CP tests of the associated quantum dynamical maps. We have applied these methods to calculate the Kossakowski matrices, and establish the CP property of the quantum dynamical evolution under the partial secular Bloch-Redfield QME of the three-level V and  $\Lambda$  systems driven by isotropic incoherent radiation.

These approaches are general in the sense that they do not require one to specify an operator form of the QME, and could be applied in a straightforward manner to many interesting QMEs, such as those, which occur in quantum thermodynamics [16–20, 22–24, 64], photosynthetic energy transfer [30–34], and spectroscopy [25–29]. All that is required in the Liouvillian matrix, which can be expressed in terms of relaxation and decoherence rates available either from experiments or via microscopic system-bath models [1, 2]. This will enable one to readily

identify the regimes, in which the CP condition breaks down, and to apply the recently developed regularization methods [12–14] to restore CP evolution. An extension of this approach to non-Markovian QMEs [82–84] could also be fruitful.

## Acknowledgements

The author is grateful to Michael Hall for bringing Ref. [51] and Eq. (3) to his attention, and to Suyesh Koyu, Amro Dodin, Paul Brumer, Mikhail Lemeshko, and Johannes Feist for stimulating discussions. This work was partially supported by the NSF CAREER program (grant No. PHY-2045681).

## A Derivation of Eq. (9) of the main text

To derive Eq. (9) of the main text, we begin by using the identity  $\mathbf{F}_m \mathbf{F}_n = \frac{1}{N} \mathbf{F}_0 \delta_{mn} + \frac{i}{2} \sum_{l=1}^M z_{mnl}^* \mathbf{F}_l$ , where  $z_{mnl} = f_{mnl} + id_{mnl}$ , and

$$\begin{aligned} f_{ijk} &= -i \text{Tr}(\{\mathbf{F}_i, \mathbf{F}_j\} \mathbf{F}_k), \\ d_{ijk} &= \text{Tr}(\{\mathbf{F}_i, \mathbf{F}_j\} \mathbf{F}_k) \end{aligned} \quad (17)$$

are the symmetric and antisymmetric structure constants of  $SU(N)$  [1, 74]. Expressing the ele-

ments of  $\mathbf{R}$  and  $\mathbf{k}$  in terms of those of  $\mathbf{A}$  [1, 74, 75]

$$r_{sm} = \sum_{i,k=1}^M \mathcal{T}_{sm,ik} a_{ik} \quad (s, m = 1, \dots, M), \quad (18)$$

$$k_s = \frac{i}{N} \sum_{i,k=1}^M a_{ik} f_{kls} \quad (s = 1, \dots, M), \quad (19)$$

where

$$\mathcal{T}_{sm,ik} = -\frac{1}{4} \sum_{l=1}^M [(f_{mnl} + id_{mnl}) f_{kls} + (f_{klm} - id_{klm}) f_{ils}], \quad (20)$$

is an  $M^2 \times M^2$  transformation tensor  $\mathcal{T}$ , which depends only on the symmetric and antisymmetric structure constants of  $\text{SU}(N)$ . The elements of  $\mathcal{T}$  are subject to a set of constraints, which follow from the sum rules satisfied by the structure constants of  $\text{SU}(N)$  as a compact semi-simple Lie group [72]. For example, one has, for  $p = 1, \dots, M$

$$\sum_{i,k=1}^M \mathcal{T}_{sm,ik} f_{ikp} = iNd_{msp}/2. \quad (21)$$

To express the elements of the Kossakowski matrix  $a_{ik}$  in terms of the relaxation and decoherence rates ( $r_{sm}$  and  $k_s$ ), we need to solve the system of linear equations (18)-(19) for the  $a_{ik}$ . Because of the constraints such as Eq. (21), the complex square tensor  $\mathcal{T}$  is not of full rank, and hence cannot be inverted, making the solution of linear equations (18)-(19) a nontrivial task.

Note that Eq. (18) can be written as a superoperator  $\hat{\mathcal{T}}$  (or a process matrix [3]), which acts on the Kossakowski matrix to produce the rate matrix,  $\hat{\mathcal{T}}\mathbf{A} = \mathbf{R}$ . It is convenient to define vectorized (Liouville) representations [85] of the Kossakowski and rate matrices  $\mathbf{a} = \text{vec}(\mathbf{A})$  and  $\mathbf{r}_0 = \text{vec}(\mathbf{R})$ , where the components  $a_\alpha$  and  $r_{0\alpha}$  are uniquely related to the elements of  $\mathbf{A}$  and  $\mathbf{R}$ , respectively, and  $\alpha = \{ik\} = 1, \dots, M^2$  is a composite index. We can now rewrite Eq. (18) in vectorized notation as  $\mathcal{T}\mathbf{a} = \mathbf{r}_0$ , where the superoperator  $\hat{\mathcal{T}}$  is represented by a square  $M^2 \times M^2$  tensor  $\mathcal{T}$  with elements  $\mathcal{T}_{\alpha\beta}$  (note that the elements of ordinary  $M \times M$  matrices, such as  $\mathbf{A} = \{a_{ik}\}$ , are indexed by Latin letters).

Because the tensor  $\mathcal{T}$  is not of full rank (see above), the linear system  $\mathcal{T}\mathbf{a} = \mathbf{r}_0$  has infinitely many solutions. To obtain a unique solution, we need to specify  $M$  additional constraints, which

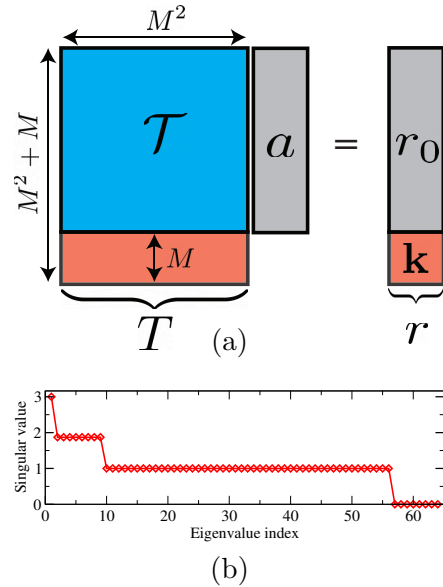


Figure 3: (a) Schematic structure of the matrix equation (23). The complex rectangular matrix of  $\text{SU}(N)$  structure constants  $\mathcal{T}$  is composed of the complex  $M^2 \times M^2$  transformation tensor  $\mathcal{T}$  given by Eq. (20) augmented by the  $M \times M^2$  matrix [see Eq. (22)]. The right-hand side consists of the vectorized rate matrix  $\mathbf{r}_0 = \text{vec}(\mathbf{R})$  augmented at the bottom by the driving vector  $\mathbf{k}$ . (b) Singular values of the tensor  $\mathcal{T}$  for  $N = 3$ . Note the presence of 8 zero singular values in the bottom right corner. The solid line is a guide to the eye.

come in the form of Eq. (19). To incorporate these constraints, we define a rectangular tensor  $\mathbf{T}$  with elements (the essential difference between the indices  $s$  and  $\beta = \{ik\}$  is noted above)

$$T_{\alpha\beta} = \mathcal{T}_{\alpha\beta} \quad (\alpha, \beta = 1, \dots, M^2),$$

$$T_{M^2+s,\beta} = \frac{i}{3} f_{sik} \quad (s = 1, \dots, M). \quad (22)$$

As illustrated in Fig. 3(a), this definition amounts to augmenting the square tensor  $\mathcal{T}$  with additional rows populated by the structure constants  $(i/3)f_{sik}$  [see Eq. (22)]. The system of linear equations (18)-(19) can then be recast in tensor form

$$\mathbf{T}\mathbf{a} = \mathbf{r}, \quad (23)$$

where  $\mathbf{r}$  is an augmented vectorized rate matrix with  $r_\alpha = r_{0\alpha} = r_{ik}$  for  $\alpha = 1, \dots, M^2$  and  $r_{M^2+s} = k_s$  [see Eqs. (18)-(19)].

The  $(M^2 + M) \times M^2$  complex rectangular tensor  $\mathbf{T}$  has rank  $M^2$ , and thus the vectorized Kossakowski matrix  $\mathbf{a} = \text{vec}(\mathbf{A})$  can be obtained as

$$\mathbf{a} = \mathbf{T}^+ \mathbf{r}, \quad (24)$$



where

$$\mathbf{T}^+ = (\mathbf{T}^\dagger \mathbf{T})^{-1} \mathbf{T}^\dagger \quad (25)$$

is the Moore-Penrose pseudo-inverse of  $\mathbf{T}$  [76–78] (the superscript  $+$  should not be confused with that for Hermitian conjugation,  $\dagger$ ). Equation (24) gives the Kossakowski matrix  $\mathbf{a} = \text{vec}(\mathbf{A})$  in terms of the relaxation and decoherence rates of a general-form QME encapsulated in  $\mathbf{r}$ .

To obtain the rate matrix  $\mathbf{R}$  and the driving vector  $\mathbf{k}$  for the three-level V-system, we first define the eight-component coherence vector  $\mathbf{v} = \sqrt{2}(\rho_{12}^R, -\rho_{12}^I, \frac{1}{2}(\rho_{11} - \rho_{22}), \rho_{13}^R, -\rho_{13}^I, \rho_{23}^R, -\rho_{23}^I, \frac{1}{\sqrt{12}}(\rho_{11} + \rho_{22} - 2\rho_{33}))^T$  in terms of the density matrix elements using the SU(3) decomposition (4), and then recast the QME (10) in the form of Eq. (5), as described in Appendix B. The resulting  $8 \times 8$   $\mathbf{R}$  matrix, whose elements are expressed in terms of  $r_i$ ,  $\gamma_i$ , and  $p$  (see Appendix B), is vectorized to form the 64-component vector  $\mathbf{r}_0$ . The latter is subsequently augmented with the 8-component  $\mathbf{k}$  vector to obtain the 72-component vector  $\mathbf{r}$  on the right-hand side of Eq. (23) (see above and Fig. 1).

The elements of the transformation tensor  $\mathbf{T}$  are calculated using Eq. (22) using the structure constants for the  $\{F_i\}$  basis of SU(3) [1]. Next, the Moore-Penrose pseudo-inverse of  $\mathbf{T}$  is calculated using Eq. (25). To verify the correctness of this procedure, we calculated the singular value decomposition of the  $64 \times 64$  complex tensor  $\mathcal{T}$  shown by the blue square in Fig. 3(a)

$$\mathcal{T} = \mathbf{U} \mathbf{\Sigma} \mathbf{V}^\dagger, \quad (26)$$

where  $\mathbf{\Sigma}$  contains the singular values of  $\mathcal{T}$  and  $\mathbf{U}$  and  $\mathbf{V}$  are unitary matrices. Figure 1(b) shows that 8 of the 64 singular values of  $\mathcal{T}$  are zero. This is consistent with the expectation that the rank of  $\mathcal{T}$  is  $M^2 - M$ , with  $M$  additional constraints needed to define  $\mathbf{T}$  (note that  $M = N^2 - 1 = 8$  for the three-level system). We also verified that Eq. (23) is consistent with Eq. (164) of Ref. [1, p. 69]. To our knowledge, the authors of Refs. [1, 41] expressed the Liouvillian matrix elements in terms of the  $a_{ik}$  for  $N = 3$ , but did not perform the inversion step accomplished in this work, which gives the  $a_{ik}$  in terms of the Liouvillian matrix elements, i.e., relaxation and decoherence rates.

## B PSBR equation for the coherence vector of the V-system

To derive the equations of motion for the coherence vector, we begin with the PSBR equations (10) for the density matrix of the V-system ( $N = 3$ ) driven by incoherent radiation [52–54, 58]. We first separate these equations into their real and imaginary parts, and then form their linear combinations to match the components of the coherence vector (4). For example, the equation of motion for  $\rho_{13}$  becomes

$$\begin{aligned} \dot{\rho}_{13}^R &= -\frac{1}{2}(2r_1 + r_2 + \gamma_1)\rho_{13}^R - \frac{p}{2}(\sqrt{r_1 r_2} + \sqrt{\gamma_1 \gamma_2})\rho_{23}^R, \\ \dot{\rho}_{13}^I &= -\frac{1}{2}(2r_1 + r_2 + \gamma_1)\rho_{13}^I - \frac{p}{2}(\sqrt{r_1 r_2} + \sqrt{\gamma_1 \gamma_2})\rho_{23}^I, \end{aligned} \quad (27)$$

Multiplying these equations by  $\pm\sqrt{2}$  and using Eq. (4), we get

$$\begin{aligned} \dot{v}_4 &= \sqrt{2}\dot{\rho}_{13}^R = -\frac{1}{2}(2r_1 + r_2 + \gamma_1)\sqrt{2}\rho_{13}^R \\ &\quad - \frac{p}{2}(\sqrt{r_1 r_2} + \sqrt{\gamma_1 \gamma_2})\sqrt{2}\rho_{23}^R \\ &= -\frac{1}{2}(2r_1 + r_2 + \gamma_1)v_4 - \frac{p}{2}(\sqrt{r_1 r_2} + \sqrt{\gamma_1 \gamma_2})v_6, \end{aligned} \quad (28)$$

and

$$\begin{aligned} \dot{v}_5 &= -\sqrt{2}\dot{\rho}_{13}^I = -\frac{1}{2}(2r_1 + r_2 + \gamma_1)(-\sqrt{2})\rho_{13}^I \\ &\quad - \frac{p}{2}(\sqrt{r_1 r_2} + \sqrt{\gamma_1 \gamma_2})\rho_{23}^I \\ &= -\frac{1}{2}(2r_1 + r_2 + \gamma_1)v_5 - \frac{p}{2}(\sqrt{r_1 r_2} + \sqrt{\gamma_1 \gamma_2})v_7, \end{aligned} \quad (29)$$

Proceeding in the same way for the other components of  $\mathbf{v}$ , we obtain the dissipative part of the QME as

$$\dot{\mathbf{v}}(t) = \mathbf{R}\mathbf{v}(t) + \mathbf{k}, \quad (30)$$

where the nonzero elements of the  $8 \times 8$  rate ma-

trix  $\mathbf{R}$  are given by

$$\begin{aligned}
R_{11} &= -\bar{r} - \bar{\gamma}, \quad R_{18} = -\frac{p\sqrt{3}}{3}(3r_{12} + \gamma_{12}), \\
R_{22} &= -\bar{r} - \bar{\gamma}, \\
R_{33} &= -\bar{r} - \bar{\gamma}, \quad R_{38} = -\frac{p\sqrt{3}}{3}(3r_{12} + \gamma_{12}), \\
R_{44} &= -\frac{1}{2}(2r_1 + r_2 + \gamma_1), \quad R_{46} = -\frac{p}{2}(r_{12} + \gamma_{12}), \\
R_{55} &= -\frac{1}{2}(2r_1 + r_2 + \gamma_1), \quad R_{57} = -\frac{p}{2}(r_{12} + \gamma_{12}), \\
R_{64} &= -\frac{p}{2}(r_{12} + \gamma_{12}), \quad R_{66} = -\frac{1}{2}(r_1 + 2r_2 + \gamma_2), \\
R_{75} &= -\frac{p}{2}(r_{12} + \gamma_{12}), \quad R_{77} = -\frac{1}{2}(r_1 + 2r_2 + \gamma_2), \\
R_{81} &= -p\sqrt{3}(r_{12} + \gamma_{12}), \quad R_{88} = -3\bar{r} - \bar{\gamma}, \\
R_{83} &= -\frac{\sqrt{3}}{2}[-(r_1 + \gamma_1) + r_2 + \gamma_2], \quad (31)
\end{aligned}$$

where  $\gamma_{12} = \sqrt{\gamma_1\gamma_2}$ ,  $r_{12} = \sqrt{r_1r_2}$ ,  $\bar{r} = \frac{1}{2}(r_1 + r_2)$ , and  $\bar{\gamma} = \frac{1}{2}(\gamma_1 + \gamma_2)$ . Finally, the driving vector  $\mathbf{k}$  is given by

$$\mathbf{k} = \begin{pmatrix} -\frac{p\sqrt{2}}{3}\gamma_{12} \\ 0 \\ -\frac{1}{3\sqrt{2}}(\gamma_1 - \gamma_2) \\ 0 \\ 0 \\ 0 \\ 0 \\ -\frac{1}{\sqrt{6}}(\gamma_1 + \gamma_2) \end{pmatrix}. \quad (32)$$

## References

- [1] R. Alicki and K. Lendi, *Quantum Dynamical Semigroups and Applications*, Lect. Notes Phys. **717** (Springer, Berlin Heidelberg, 2007).
- [2] H.-P. Breuer and F. Petruccione, *The Theory of Open Quantum Systems* (Clarendon Press, Oxford, 2006).
- [3] M. A. Nielsen and I. L. Chuang, *Quantum Computation and Quantum Information: 10th Anniversary Edition* (Cambridge University Press, 2010).
- [4] F. Campaioli, J. H. Cole, and H. Haruarachchi, Quantum master equations: Tips and tricks for quantum optics, quantum computing, and beyond, *PRX Quantum* **5**, 020202 (2024).
- [5] G. McCauley, B. Cruikshank, D. I. Bondar, and K. Jacobs, Accurate Lindblad-form master equation for weakly damped quantum systems across all regimes, *npj Quantum Information* **6**, 74 (2020).
- [6] D. Davidović, Completely Positive, Simple, and Possibly Highly Accurate Approximation of the Redfield Equation, *Quantum* **4**, 326 (2020).
- [7] E. Mozgunov and D. Lidar, Completely positive master equation for arbitrary driving and small level spacing, *Quantum* **4**, 227 (2020).
- [8] D. Manzano, A short introduction to the Lindblad master equation, *AIP Adv.* **10**, 025106 (2020).
- [9] P. Groszkowski, A. Seif, J. Koch, and A. A. Clerk, Simple master equations for describing driven systems subject to classical non-Markovian noise, *Quantum* **7**, 972 (2023).
- [10] V. V. Albert and L. Jiang, Symmetries and conserved quantities in Lindblad master equations, *Phys. Rev. A* **89**, 022118 (2014).
- [11] V. V. Albert, B. Bradlyn, M. Fraas, and L. Jiang, Geometry and response of Lindbladians, *Phys. Rev. X* **6**, 041031 (2016).
- [12] A. D’Abbruzzo, V. Cavina, and V. Giovannetti, A time-dependent regularization of the Redfield equation, *SciPost Phys.* **15**, 117 (2023).
- [13] A. D’Abbruzzo, D. Farina, and V. Giovannetti, Recovering complete positivity of non-Markovian quantum dynamics with Choi-proximity regularization, *Phys. Rev. X* **14**, 031010 (2024).
- [14] D. Fernández de la Pradilla, E. Moreno, and J. Feist, Recovering an accurate Lindblad equation from the Bloch-Redfield equation for general open quantum systems, *Phys. Rev. A* **109**, 062225 (2024).
- [15] M. O. Scully and M. Zubairy, *Quantum Optics* (Cambridge University Press, 1997).
- [16] F. Binder, L. A. Correa, C. Gogolin, J. Anders, and G. Adesso, eds., *Thermodynamics in the Quantum Regime: Fundamental Aspects and New Directions* (Springer, Berlin, 2018).
- [17] R. Alicki, The quantum open system as a model of the heat engine, *J. Phys. A* **12**, L103 (1979).
- [18] R. Kosloff, Quantum thermodynamics and open-systems modeling, *J. Chem. Phys.* **150**, 204105 (2019).

- [19] P. P. Potts, *Quantum Thermodynamics*, SciPost Phys. Lecture Notes, [arXiv:2406.19206](https://arxiv.org/abs/2406.19206) (2024).
- [20] J. Liu and D. Segal, Coherences and the thermodynamic uncertainty relation: Insights from quantum absorption refrigerators, *Phys. Rev. E* **103**, 032138 (2021).
- [21] S. Scali, J. Anders, and L. A. Correa, Local master equations bypass the secular approximation, *Quantum* **5**, 451 (2021).
- [22] N. M. Myers, O. Abah, and S. Deffner, Quantum thermodynamic devices: From theoretical proposals to experimental reality, *AVS Quant. Sci.* **4**, 027101 (2022).
- [23] A. Soret, V. Cavina, and M. Esposito, Thermodynamic consistency of quantum master equations, *Phys. Rev. A* **106**, 062209 (2022).
- [24] O. Onishchenko, G. Guarnieri, P. Rosillo-Rodes, D. Pijn, J. Hilder, U. G. Poschinger, M. Perarnau-Llobet, J. Eisert, and F. Schmidt-Kaler, Probing coherent quantum thermodynamics using a trapped ion, *Nat. Commun.* **15**, 6974 (2024).
- [25] J. Yuen-Zhou, J. J. Krich, M. Mohseni, and A. Aspuru-Guzik, Quantum state and process tomography of energy transfer systems via ultrafast spectroscopy, *Proc. Natl. Acad. Sci. USA* **108**, 17615 (2011).
- [26] T. Mančal and F. Šanda, Quantum master equations for non-linear optical response of molecular systems, *Chem. Phys. Lett.* **530**, 140 (2012).
- [27] J. Yuen-Zhou, J. J. Krich, I. Kassal, A. S. Johnson, and A. Aspuru-Guzik, *Ultrafast Spectroscopy. Quantum information and wavepackets* (IOP Publishing, 2014).
- [28] J. H. Fetherolf and T. C. Berkelbach, Linear and nonlinear spectroscopy from quantum master equations, *J. Chem. Phys.* **147**, 244109 (2017).
- [29] T. Sayer and A. Montoya-Castillo, Efficient formulation of multitime generalized quantum master equations: Taming the cost of simulating 2D spectra, *J. Chem. Phys.* **160**, 044108 (2024).
- [30] P. Rebentrost, M. Mohseni, and A. Aspuru-Guzik, Role of quantum coherence and environmental fluctuations in chromophoric energy transport, *J. Phys. Chem. B* **113**, 9942 (2009).
- [31] J. Cao and R. J. Silbey, Optimization of excitation trapping in energy transfer processes, *J. Phys. Chem. A* **113**, 13825 (2009).
- [32] M. F. Gelin, D. Egorova, and W. Domcke, Exact quantum master equation for a molecular aggregate coupled to a harmonic bath, *Phys. Rev. E* **84**, 041139 (2011).
- [33] R. d. J. León-Montiel, I. Kassal, and J. P. Torres, Importance of excitation and trapping conditions in photosynthetic environment-assisted energy transport, *J. Phys. Chem. B* **118**, 10588 (2014).
- [34] T. V. Tscherbul and P. Brumer, Non-equilibrium stationary coherences in photosynthetic energy transfer under weak-field incoherent illumination, *J. Chem. Phys.* **148**, 124114 (2018).
- [35] F. Benatti, R. Floreanini, and R. Romano, Complete positivity and entangled degrees of freedom, *J. Phys. A* **35**, 4955 (2002).
- [36] F. Benatti, D. Chruściński, and R. Floreanini, Local generation of entanglement with Redfield dynamics, [arXiv:2206.04508v1](https://arxiv.org/abs/2206.04508v1) (2022).
- [37] G. Argentieri, F. Benatti, R. Floreanini, and M. Pezzutto, Violations of the second law of thermodynamics by a non-completely positive dynamics, *Europhys. Lett.* **107**, 50007 (2014).
- [38] Y. Wang, Z. Hu, B. C. Sanders, and S. Kais, Qudits and high-dimensional quantum computing, *Front. Phys.* **8**, 589504 (2020).
- [39] Y. Chi, J. Huang, Z. Zhang, J. Mao, Z. Zhou, X. Chen, C. Zhai, J. Bao, T. Dai, H. Yuan, M. Zhang, D. Dai, B. Tang, Y. Yang, Z. Li, Y. Ding, L. K. Oxenløwe, M. G. Thompson, J. L. O'Brien, Y. Li, Q. Gong, and J. Wang, A programmable qudit-based quantum processor, *Nat. Commun.* **13**, 1166 (2022).
- [40] A. Rivas, S. F. Huelga, and M. B. Plenio, Entanglement and non-Markovianity of quantum evolutions, *Phys. Rev. Lett.* **105**, 050403 (2010).
- [41] J. Pöttinger, Master's thesis, University of Zürich (1983).
- [42] D. Farina and V. Giovannetti, Open-quantum-system dynamics: Recovering positivity of the Redfield equation via the partial secular approximation, *Phys. Rev. A* **100**, 012107 (2019).
- [43] A. Trushechkin, Unified Gorini-

- Kossakowski-Lindblad-Sudarshan quantum master equation beyond the secular approximation, *Phys. Rev. A* **103**, 062226 (2021).
- [44] B. Vacchini, Generalized master equations leading to completely positive dynamics, *Phys. Rev. Lett.* **117**, 230401 (2016).
- [45] E. Andersson, J. D. Cresser, and M. J. W. Hall, Finding the Kraus decomposition from a master equation and vice versa, *J. Mod. Opt.* **54**, 1695 (2007).
- [46] M.-D. Choi, Completely positive linear maps on complex matrices, *Linear Algebra Appl.* **10**, 285 (1975).
- [47] H.-P. Breuer, B. Kappler, and F. Petruccione, The time-convolutionless projection operator technique in the quantum theory of dissipation and decoherence, *Ann. Phys.* **291**, 36 (2001).
- [48] F. Shibata, Y. Takahashi, and N. Hashitsume, A generalized stochastic liouville equation. Non-Markovian versus memoryless master equations, *J. Stat. Phys.* **17**, 171 (1977).
- [49] S. Chaturvedi and F. Shibata, Time-convolutionless projection operator formalism for elimination of fast variables. Applications to Brownian motion, *Z. Phys. B* **35**, 297 (1979).
- [50] C. M. Caves, Quantum error correction and reversible operations, *J. Supercond.* **12**, 707 (1999).
- [51] M. J. W. Hall, J. D. Cresser, L. Li, and E. Andersson, Canonical form of master equations and characterization of non-Markovianity, *Phys. Rev. A* **89**, 042120 (2014).
- [52] V. V. Kozlov, Y. Rostovtsev, and M. O. Scully, Inducing quantum coherence via decays and incoherent pumping with application to population trapping, lasing without inversion, and quenching of spontaneous emission, *Phys. Rev. A* **74**, 063829 (2006).
- [53] T. V. Tscherbul and P. Brumer, Long-lived quasistationary coherences in a V-type system driven by incoherent light, *Phys. Rev. Lett.* **113**, 113601 (2014).
- [54] T. V. Tscherbul and P. Brumer, Partial secular Bloch-Redfield master equation for incoherent excitation of multilevel quantum systems, *J. Chem. Phys.* **142**, 104107 (2015).
- [55] K. Beloy, U. I. Safronova, and A. Derevianko, High-accuracy calculation of the blackbody radiation shift in the  $^{133}\text{Cs}$  primary frequency standard, *Phys. Rev. Lett.* **97**, 040801 (2006).
- [56] A. Dodin, T. V. Tscherbul, and P. Brumer, Population oscillations and ubiquitous coherences in multilevel quantum systems driven by incoherent radiation, *J. Phys. Chem. Lett.* **15**, 7694 (2024).
- [57] I. Kassal, J. Yuen-Zhou, and S. Rahimi-Keshari, Does coherence enhance transport in photosynthesis?, *J. Phys. Chem. Lett.* **4**, 362 (2013).
- [58] A. Dodin, T. V. Tscherbul, and P. Brumer, Quantum dynamics of incoherently driven V-type systems: Analytic solutions beyond the secular approximation, *J. Chem. Phys.* **144**, 244108 (2016).
- [59] A. Dodin, T. V. Tscherbul, R. Alicki, A. Vutha, and P. Brumer, Secular versus nonsecular Redfield dynamics and Fano coherences in incoherent excitation: An experimental proposal, *Phys. Rev. A* **97**, 013421 (2018).
- [60] S. Koyu and T. V. Tscherbul, Long-lived quantum coherences in a V-type system strongly driven by a thermal environment, *Phys. Rev. A* **98**, 023811 (2018).
- [61] S. Koyu, A. Dodin, P. Brumer, and T. V. Tscherbul, Steady-state Fano coherences in a V-type system driven by polarized incoherent light, *Phys. Rev. Res.* **3**, 013295 (2021).
- [62] S. Koyu and T. V. Tscherbul, Long-lived quantum coherent dynamics of a  $\Lambda$ -system driven by a thermal environment, *J. Chem. Phys.* **157**, 124302 (2022).
- [63] P. Brumer, Shedding (incoherent) light on quantum effects in light-induced biological processes, *J. Phys. Chem. Lett.* **9**, 2946 (2018).
- [64] M. O. Scully, K. R. Chapin, K. E. Dorfman, M. B. Kim, and A. Svidzinsky, Quantum heat engine power can be increased by noise-induced coherence, *Proc. Natl. Acad. Sci. USA* **108**, 15097 (2011).
- [65] K. E. Dorfman, D. V. Voronine, S. Mukamel, and M. O. Scully, Photosynthetic reaction center as a quantum heat engine, *Proc. Natl. Acad. Sci. USA* **110**, 2746 (2013).
- [66] G. S. Agarwal and S. Menon, Quantum in-

- interferences and the question of thermodynamic equilibrium, *Phys. Rev. A* **63**, 023818 (2001).
- [67] M. Merkli, H. Song, and G. P. Berman, Multiscale dynamics of open three-level quantum systems with two quasi-degenerate levels, *J. Phys. A* **48**, 275304 (2015).
- [68] F. Ivander, N. Anto-Sztrikacs, and D. Segal, Hyperacceleration of quantum thermalization dynamics by bypassing long-lived coherences: An analytical treatment, *Phys. Rev. E* **108**, 014130 (2023).
- [69] M. Gerry, M. J. Kewming, and D. Segal, Understanding multiple timescales in quantum dissipative dynamics: Insights from quantum trajectories, *Phys. Rev. Res.* **6**, 033106 (2024).
- [70] N. Anto-Sztrikacs, H. J. D. Miller, A. Nazir, and D. Segal, Bypassing thermalization timescales in temperature estimation using prethermal probes, *Phys. Rev. A* **109**, L060201 (2024).
- [71] D. A. Lidar, I. L. Chuang, and K. B. Whaley, Decoherence-free subspaces for quantum computation, *Phys. Rev. Lett.* **81**, 2594 (1998).
- [72] A. J. Macfarlane, A. Sudbery, and P. H. Weisz, On Gell-Mann's  $\lambda$ -matrices,  $d$  and  $f$ -tensors, octets, and parametrizations of  $SU(3)$ , *Comm. Math. Phys.* **11**, 77 (1968).
- [73] V. Gorini, A. Kossakowski, and E. C. G. Sudarshan, Completely positive dynamical semigroups of  $N$ -level systems, *J. Math. Phys.* **17**, 821 (1976).
- [74] K. Lendi, Evolution matrix in a coherence vector formulation for quantum Markovian master equations of  $N$ -level systems, *J. Phys. A* **20**, 15 (1987).
- [75] J. Pöttinger and K. Lendi, Generalized Bloch equations for decaying systems, *Phys. Rev. A* **31**, 1299 (1985).
- [76] E. H. Moore, On the reciprocal of the general algebraic matrix, *Bull. Am. Math. Soc.* **26**, 394 (1920).
- [77] R. Penrose, A generalized inverse for matrices, *Math. Proc. Camb. Philos. Soc.* **51**, 406 (1955).
- [78] J. C. A. Barata and M. S. Hussein, The Moore–Penrose pseudoinverse: A tutorial review of the theory, *Braz. J. Phys.* **42**, 146 (2012).
- [79] S. Koyu, *Noise-induced Coherent Dynamics of Multilevel Quantum Systems Driven by Incoherent Light: A Case Study of the Three-level V-system*, *Ph.D. thesis*, University of Nevada, Reno (2020).
- [80] L. Donati, F. S. Cataliotti, and S. Gherardini, Energetics and quantumness of Fano coherence generation, *Sci. Rep.* **14**, 20145 (2024).
- [81] B.-Q. Ou, L.-M. Liang, and C.-Z. Li, Coherence induced by incoherent pumping field and decay process in three-level  $\Lambda$ -type atomic system, *Opt. Commun.* **281**, 4940 (2008).
- [82] H.-P. Breuer, E.-M. Laine, J. Piilo, and B. Vacchini, Colloquium: Non-Markovian dynamics in open quantum systems, *Rev. Mod. Phys.* **88**, 021002 (2016).
- [83] I. de Vega and D. Alonso, Dynamics of non-Markovian open quantum systems, *Rev. Mod. Phys.* **89**, 015001 (2017).
- [84] D. Chruściński, Dynamical maps beyond Markovian regime, *Phys. Rep.* **992**, 1 (2022).
- [85] J. A. Gyamfi, Fundamentals of quantum mechanics in Liouville space, *Eur. J. Phys.* **41**, 063002 (2020).